ISSN 1070-3284, Russian Journal of Coordination Chemistry, 2023, Vol. 49, No. 4, pp. 206–217. © Pleiades Publishing, Ltd., 2023.
Russian Text © The Author(s), 2023, published in Koordinatsionnaya Khimiya, 2023, Vol. 49, No. 4, pp. 205–216.

Preparation of Water-Soluble Zinc(II) Complexes with Ethylenediaminetetraacetic Acid: Molecular Structure of Zinc Ethylenediaminetetraacetate Trihydrate

V. V. Semenov[a, *], N. V. Zolotareva[a], O. V. Novikova[a], B. I. Petrov[a], N. M. Lazarev[a], R. V. Rumyantsev[a], M. A. Lopatin[a], T. I. Lopatina[a], T. A. Kovylina[a], and E. N. Razov[b, c]

[a] *Razuvaev Institute of Organometallic Chemistry, Russian Academy of Sciences, Nizhny Novgorod, Russia*

[b] *Lobachevsky State University of Nizhny Novgorod, Nizhny Novgorod, Russia*

[c] *Institute of Problems of Mechanical Engineering, Russian Academy of Sciences—A Branch of the Federal Research Center, Institute of Applied Physics, Russian Academy of Sciences, Nizhny Novgorod, Russia*

**e-mail: vvsemenov@iomc.ras.ru*

Received June 28, 2022; revised October 16, 2022; accepted November 2, 2022

Abstract—Poorly soluble zinc ethylenediaminetetraacetate zincate Zn[ZnL] reacts with sodium Na_4L, potassium K_4L, ammonium $(NH_4)_4L$, 2-ammonioethanol $(H_3NCH_2CH_2OH)_4L$, and hexamethylene-1,6-diammonium $\{H_3N(CH_2)_6NH_3\}_2L$ salts of ethylenediaminetetraacetic acid H_4L to give readily soluble sodium $Na_2[ZnL]$, potassium $K_2[ZnL]$, ammonium $(NH_4)_2[ZnL]$, 2-ammonioethanol $(H_3NCH_2CH_2OH)_2[ZnL]$, and hexamethylene-1,6-diammonium $\{H_3N(CH_2)_6NH_3\}[ZnL]$ ethylenediaminetetraacetate zincates. The reaction of tetrakis(triethylammonium) salt $\{(C_2H_5)_3NH\}_4L$ with Zn[ZnL] does not give the expected bis(triethylammonium) ethylenediaminetetraacetate zincate $\{(C_2H_5)_3NH\}_2[ZnL]$, but gives instead mono(triethylammonium) ethylenediaminetetraacetate zincate, $\{(C_2H_5)_3NH\}H[ZnL]$; in aqueous solution, this product generates poorly soluble zinc ethylenediaminetetraacetate $H_2[ZnL(H_2O)]\cdot 2H_2O$, which was studied by X-ray diffraction (CCDC no. 2172274).

Keywords: salts of ethylenediaminetetraacetic acid, 2-aminoethanol, hexamethylene-1,6-diamine, triethylamine, ammonium ethylenediaminetetraacetate zincates, zinc complexes, molecular structure

DOI: 10.1134/S1070328423700434

INTRODUCTION

Zinc coordination compounds based on commercial chelating agents with carboxyl and phosphonic groups are used [1] in medicine, agriculture, and mechanical engineering. Practical applications require, most often, aqueous solutions. Meanwhile, many of known compounds are poorly soluble. Alkali metal derivatives are readily soluble. Complexes of 3*d* metals with phosphonic ligands usually have better solubility than those with carboxyl-containing ligands. High ligand denticity is favorable for higher solubility. The so-called solubility promoters [2] are amines with hydroxyl or oligo(ethylene oxide) groups. Among them, most readily available are water-soluble mono-, di-, and triethanolamines, which are industrially manufactured. When they add to a chelate, it is easily transferred to the aqueous phase. The addition can occur not only at the metal cation, but also at the remaining free acid groups.

$$RC(O)OH + H_2NCH_2CH_2OH \rightarrow RC(O)O^{-}{}^{+}H_3NCH_2CH_2OH,$$

$$RP(O)OH + H_2NCH_2CH_2OH \rightarrow RP(O)O^{-}{}^{+}H_3NCH_2CH_2OH.$$

It was shown [3] that chelates can be transferred to the aqueous phase by treatment with amines containing no hydrophilic groups (triethylamine, tributylamine, or *tert*-butylamine). This effect is due to the destruction of the coordination polymer. Here we studied the reactions of zinc oxide with ethylenediaminetetraacetic acid (EDTA, H_4L) and the subsequent transformations of the products. In the crystalline state and in solution, EDTA has a betaine structure [1].

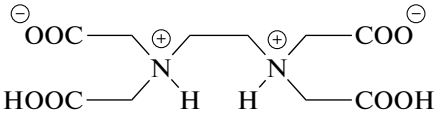

(H_4L)

The complex formation of zinc with EDTA was studied by spectrophotometry [4], polarography [5], and by differential pulse voltammetry [6]. The kinetics

of zinc(II) substitution in zinc EDTA complex was studied by radioisotope exchange [7]. The applicability of zinc ethylenediaminetetraacetate as a food supplement in animal feed was tested [8]. Zinc uptake and transfer from zinc-contaminated soil by the root shoots of plants in the presence of increasing EDTA concentrations in soil were studied in relation to barley, potatoes, mustard, and lupine [9, 10].

EXPERIMENTAL

Commercial high-purity grade EDTA disodium salt (Trilon B) (JSC Khimreaktiv, Nizhny Novgorod) and high-purity grade 2-aminoethanol (LLC Sintez OKA, Dzerzhinsk) were used; EDTA was prepared by treating the disodium salt with HCl.

Synthesis of zinc(II) ethylenediaminetetraacetate zincate dihydrate $Zn[ZnL]\cdot 2H_2O$ (I). EDTA (5.00 g, 1.72×10^{-2} mol) and ZnO (2.80 g, 3.45×10^{-2} mol) were mixed and ground in a mortar. The white powder that formed was poured with stirring into H_2O (50 mL). The suspension dissolved within 15 min. The mixture was concentrated, and the residue was dried at 110°C, mixed with H_2O (200 mL), heated to boiling, and filtered while hot. The precipitate on the filter was dried at 110°C. Compound **I** was formed in 5.15 g yield as a white mass easily breaking up into a white powder.

IR (ν, cm^{-1}): 3300, 3026, 1694, 1611, 1584, 1450, 1420, 1402, 1388, 1331, 1310, 1286, 1262, 1239, 1125, 1107, 1006, 981, 970, 935, 920, 866, 815, 771, 726, 661, 619, 586, 562, 532, 503, 470.

For $C_{10}H_{20}N_2O_{10}Zn_2$ (**I**)

Anal. calcd., %	C, 26.16	H, 4.39	N, 6.10
Found, %	C, 26.41	H, 3.93	N, 6.02

The filtrate was concentrated, and the residue was dried at 110°C. The additional yield of **I** was 1.80 g, and the total yield was 6.95 g (1.51×10^{-2} mol, 88%). The solubility of **I** was 0.98 g in 100 mL of H_2O at 80°C.

Synthesis of $Na_2[ZnL]$ (II). EDTA (5.00 g, 1.72×10^{-2} mol) and ZnO (2.80 g, 3.45×10^{-2} mol) were mixed and ground in a mortar. The white powder that formed was poured with stirring into H_2O (50 mL). The suspension dissolved within 20 min. The salt Na_2H_2L (6.40 g, 1.72×10^{-2} mol) was added to the reaction mixture in small portions, and then a solution of NaOH (1.40 g, 3.44×10^{-2} mol) in H_2O (10 mL) was added dropwise. The resulting transparent colorless solution (pH 6) was concentrated, and the residue was dried at 110°C. Compound **II** was formed in a yield of 13.50 g (3.38×10^{-2} mol, 98%) as a white soft powder.

IR (ν, cm^{-1}): 3583, 3446, 3363, 3285, 1614, 1590, 1459, 1435, 1393, 1322, 1292, 1247, 1173, 1110, 1006, 979, 964, 860, 842, 804, 762, 720, 658, 640, 583, 538, 515, 467.

For $C_{10}H_{12}N_2O_8Na_2Zn$ (**II**)

Anal. calcd., %	C, 30.06	H, 3.03	N, 7.01
Found, %	C, 30.55	H, 3.56	N, 7.14

Synthesis of $K_2[ZnL]\cdot H_2O$ (III). EDTA (5.00 g, 1.72×10^{-2} mol) and ZnO (2.80 g, 3.45×10^{-2} mol) were mixed and ground in a mortar. The white powder that formed was poured with stirring into H_2O (50 mL). After 20 min, a solution (30 mL) of salt K_4L, prepared from EDTA (5.00 g, 1.72×10^{-2} mol) and KOH (3.86 g, 6.88×10^{-2} mol), was added to the reaction mixture. After 12 h, a precipitate was formed in the transparent mixture. The mixture was concentrated, and the residue was dried at 110°C. Compound **III** was formed in a yield of 13.00 g (3.01×10^{-2} mol, 88%) as a white firm solid mass breaking up into a white powder. Very small crystals shaped like short rods precipitated from the supersaturated aqueous solution.

IR (ν, cm^{-1}): 3607 sh, 3402 br, 1718 sh, 1614, 1593, 1447, 1402, 1325, 1307, 1280, 1268, 1110, 1003, 979, 932, 854, 717, 640, 595, 532, 506, 461.

For $C_{10}H_{14}N_2O_9K_2Zn$ (**III**)

Anal. calcd., %	C, 26.70	H, 3.14	N, 6.23
Found, %	C, 26.77	H, 3.45	N, 6.48

Synthesis of $(NH_4)_2[ZnL]\cdot H_2O$ (IV). EDTA (5.00 g, 1.72×10^{-2} mol) and ZnO (2.80 g, 3.45×10^{-2} mol) were mixed and ground in a mortar. The white powder that formed was poured with stirring into H_2O (50 mL). After 20 min a solution (20 mL) of $(NH_4)_4L$, prepared from EDTA (5.00 g, 1.72×10^{-2} mol) and a 10.37 M solution of NH_4OH (6.63 mL, 6.88×10^{-2} mol), was added to the reaction mixture. After 12 h, the mixture was filtered, the filtrate was concentrated, and the residue was dried at 110°C. Compound **IV** was formed in a yield of 11.80 g (3.03×10^{-2} mol, 95%) as a soft white powder. Small needle-shaped crystals precipitated from a supersaturated aqueous solution.

IR (ν, cm^{-1}): 3440, 3214, 1709, 1590, 1459, 1444, 1396, 1331, 1319, 1310, 1268, 1247, 1221, 1173, 1110, 1006, 976, 935, 917, 854, 810, 768, 723, 646, 610, 589, 538, 506, 461.

For $C_{10}H_{22}N_4O_9Zn$ (**IV**)

Anal. calcd., %	C, 29.46	H, 5.44	N, 13.74
Found, %	C, 29.49	H, 5.41	N, 13.24

Reaction of $Zn[ZnL]\cdot 2H_2O$ with 2-aminoethanol. $H_2NCH_2CH_2OH$ (1.22 g, 2.00×10^{-2} mol) in H_2O (10 mL) was added dropwise to a suspension of

$Zn[ZnL]\cdot 2H_2O$ (4.60 g, 1.00×10^{-2} mol) in H_2O (30 mL). The mixture was stirred at reflux for 1 h, cooled, and filtered, and the residue was washed with methanol and dried at 110°C to give 1.30 g of a solid mass breaking up into a white powder. The filtrate was concentrated, and the residue was dried at 110°C. Compound $(H_3NCH_2CH_2OH)_2[ZnL]$ (**V**) formed in a yield of 3.80 g (7.95×10^{-3} mol, 79%) as a white foam breaking up into a white powder.

IR (ν, cm^{-1}): 3500–2200 br, 1727, 1599, 1459, 1393, 1379, 1319, 1274, 1221, 1113, 1066, 1015, 1006, 970, 920, 860, 723, 649, 595, 515, 467.

For $C_{14}H_{28}N_4O_{10}Zn$

Anal. calcd., %	C, 35.19	H, 5.91	N, 11.73
Found, %	C, 35.69	H, 5.89	N, 11.98

Synthesis of 2-ammonioethanol ethylenediaminetetraacetate zincate $(H_3NCH_2CH_2OH)_2[ZnL]$ (V). EDTA (5.00 g, 1.72×10^{-2} mol) and ZnO (2.80 g, 3.45×10^{-2} mol) were mixed and ground in a mortar. The white powder that formed was poured with stirring into H_2O (30 mL). After 20 min, a solution (20 mL) of $(NH_3CH_2CH_2OH)_4L$, prepared from EDTA (5.00 g, 1.72×10^{-2} mol) and 2-aminoethanol (4.20 g, 6.88×10^{-2} mol), was added to the reaction mixture. The mixture was filtered, the filtrate was concentrated, and the residue was dried at 110°C. This gave 16.60 g of a light yellow wax that melted on heating to 100°C. After heating in vacuum to 175°C, the yield of **V**, formed as a loose foam breaking up into a white powder, was 13.00 g (2.72×10^{-2} mol, 79%). The compound was moderately soluble in methanol and formed a transparent colorless film on glass; it was insoluble in dioxane, acetone, and acetonitrile, and could not be reprecipitated from aqueous solutions upon the addition of the above-mentioned organic solvents.

IR (ν, cm^{-1}): 3279, 3086, 1733, 1587, 1459, 1390, 1379, 1322, 1310, 1274, 1221, 1176, 1116, 1069, 1015, 1003, 973, 923, 860, 810, 723, 649, 592, 518, 467.

For $C_{14}H_{28}N_4O_{10}Zn$ (**V**)

Anal. calcd., %	C, 35.19	H, 5.91	N, 11.73
Found, %	C, 36.09	H, 5.79	N, 11.90

Synthesis of hexamethylene-1,6-diammonium ethylenediaminetetraacetate zincate $\{H_3N(CH_2)_6NH_3\}[ZnL]$ (VI). EDTA (5.24 g, 1.81×10^{-2} mol) and ZnO (2.94 g, 3.61×10^{-2} mol) were mixed and ground in a mortar. The white powder that formed was poured with stirring into H_2O (30 mL). After 20 min, a solution of $\{H_3N(CH_2)_6NH_3\}_2L$, prepared from EDTA (5.24 g, 1.81×10^{-2} mol) and hexamethylene-1,6-diamine (4.20 g, 3.61×10^{-2} mol) in H_2O (20 mL), was added to the reaction mixture. The mixture was filtered, the filtrate was concentrated, and the residue was dried at 110°C. This gave 16.90 g of a solid mass, which softened on heating to 100°C. After heating in vacuum to 165°C, **VI** was formed in a yield of 14.15 g (3.00×10^2 mol, 83%) as large light yellow pieces breaking up into a cream powder.

IR (ν, cm^{-1}): 3443, 3133, 3000–2200 br, 2091, 1602, 1483, 1462, 1390, 1379, 1325, 1271, 1173, 1110, 1000, 964, 917, 863, 839, 723, 658, 625, 589, 550, 509, 461.

For $C_{16}H_{30}N_4O_8Zn$ (**VI**)

Anal. calcd., %	C, 40.73	H, 6.41	N, 11.87
Found, %	C, 41.38	H, 7.01	N, 11.81

The compound was soluble in methanol and ethylene glycol, poorly soluble in acetonitrile and DMSO, and insoluble in acetone. From methanol solution, a transparent film of the product was formed on glass.

Synthesis of triethylammonium ethylenediaminetetraacetate zincate hydrate $\{(C_2H_5)_3NH\}H[ZnL]\cdot H_2O$ (VII). EDTA (5.00 g, 1.72×10^{-2} mol) and ZnO (2.80 g, 3.45×10^{-2} mol) were mixed and ground in a mortar. The white powder that formed was poured with stirring into H_2O (30 mL). After 20 min, a solution of $\{(C_2H_5)_3NH\}_4L$, prepared from EDTA (5.00 g, 1.72×10^{-2} mol) and triethylamine (6.96 g, 6.88×10^{-2} mol) in H_2O (20 mL), was added to the reaction mixture. The mixture was filtered, the filtrate was concentrated, and the residue was dried at 110°C. This gave 14.90 g of a white mass, which could be broken up into a white powder with difficulty. After heating of the powder in vacuum to 150°C, the yield of **VII** was 14.30 g (2.56×10^{-2} mol, 74%).

IR (ν, cm^{-1}): 3583, 3476, 3378, 3294, 3011 sh, 2684, 2636, 2576, 2499, 1715, 1656, 1620, 1587, 1447, 1429, 1405, 1376, 1346, 1319, 1301, 1262, 1206, 1170, 1113, 1066, 1033, 1006, 982, 932, 917, 884, 857, 845, 810, 765, 723, 646, 589, 556, 526, 464.

For $C_{16}H_{31}N_3O_9Zn$ (**VII**)

Anal. calcd., %	C, 40.47	H, 6.58	N, 8.85
Found, %	C, 40.77	H, 6.76	N, 9.03

Synthesis of zinc ethylenediaminetetraacetate trihydrate $H_2[ZnL(H_2O)]\cdot 2H_2O$ (VIII). Water (10 mL) was saturated with $\{(C_2H_5)_3NH\}H[ZnL]\cdot H_2O$ (10.40 g, 2.19×10^{-2} mol) with stirring without heating. Large cubic crystals precipitated from the solution within 2 days. The crystals were collected on a filter, washed with methanol and acetone, and dried in air. The yield of **VIII** was 1.80 g (4.23×10^{-3} mol, 19%).

IR (ν, cm^{-1}): 3372, 3214, 2657, 2526, 2231, 1927, 1712, 1605, 1465, 1390, 1367, 1331, 1313, 1292, 1253, 1116, 1003, 970, 932, 914, 860, 726, 681, 646, 604, 562, 506, 455.

For $C_{10}H_{20}N_2O_{11}Zn$ (**VIII**)

Anal. calcd., %	C, 29.32	H, 4.92	N. 6.84
Found, %	C, 28.94	H, 5.09	N, 6.86

Synthesis of KH[ZnL] (IX). K_2[ZnL] (2.60 g, 5.78×10^{-2} mol) was added to distilled water (7 mL), the mixture was stirred, and 7 drops of 8 N H_2SO_4 were added. The mixture became thick as an abundant precipitate formed. The precipitate was collected on a filter, washed with water, and dried at 110°C. Compound **IX** was formed in a yield of 0.85 g (2.16×10^{-2} mol, 37%) as a white powder.

IR (ν, cm^{-1}): 2705, 2576, 2492, 1911, 1724, 1691, 1593, 1462, 1441, 1429, 1396, 1322, 1304, 1253, 1197, 1176, 1113, 1009, 970, 929, 908, 881, 860, 812, 759, 723, 696, 634, 598, 577, 503, 467.

For $C_{10}H_{13}N_2O_8Zn$ (**IX**)

Anal. calcd., %	C, 30.51	H, 3.33	N, 7.12
Found, %	C, 31.03	H, 3.57	N, 7.41

IR spectra were recorded on an FSM 1201 FTIR spectrometer for samples in mineral (1400–400 cm^{-1}) and fluorinated oils (4000–1400 cm^{-1}) between KBr plates. Elemental analysis was performed on a Vario EL cube automatic analyzer (Elementar Analysensysteme GmbH) in the CHNS configuration using helium 6.0 as a carrier gas. The UV–Vis spectra of aqueous solutions were measured on a Perkin-Elmer Lambda 25 spectrophotometer. Optical microscopy examination was carried out on a Mikromed 3 microscope (Ningbo Sheng Heng Optics & Electronics Co., Ltd.) with a ToupCam14MP digital camera, China; Nablyudatelnye Pribory LLC, St.-Petersburg. A Shimadzu XRD-7000 X-ray diffractometer was used for powder X-ray diffraction study. Thermogravimetric analysis **(**TGA**)** was conducted on a TGA/DSC 3+ METTLER TOLEDO simultaneous thermal analysis instrument (heating rate of 5 K/min, argon flow rate of 20 mL/min). The measurements were carried out in the temperature range from 25 to 500°C.

The mass spectra of the compounds were run using a Trace GC Ultra/Polaris Q GC/MS spectrometer (Thermo Electron Corporation, USA) equipped with a direct injection system and ion trap mass analyzer. The test compound in an amount sufficient for generating an ion current 100 times as high as the background current was rubbed into the inner surface of the standard glass crucible of the direct injection system. After preliminary evacuation, the crucible with the sample was moved with the rod to a close vicinity of the ion source. Positive ion mass spectra were measured at an ionizing energy of 70 eV in the mass number range of 50–700. The temperature of the sample was changed according to the following program: instantaneous heating to 50°C, isothermal conditions for 1 min, and heating at a rate of 100°C min^{-1} up to 450°C. The ion source temperature was 230°C.

Scanning electron microscopy (SEM) was performed on a Tescan VEGA II scanning electron microscope. The microrelief was studied at magnifications from 500× to 50000×. The measurements were carried out at an accelerating voltage of 20 kV and a working distance of 2–8 mm using secondary electron (SE) and backscattered electron (BSE) detectors.

X-ray diffraction analysis of **VIII** was carried out on an Oxford Xcalibur Eos diffractometer (graphite monochromator, MoK_α radiation, ω-scan mode, λ = 0.71073 Å) at 298(2) K. The experimental sets of intensities were integrated by the CrysAlisPro program [11]. The absorption corrections were applied using the SCALE3 ABSPACK scaling algorithm implemented in the CrysAlisPro software. The structure was solved using the SHELXT software [12] and refined by the full-matrix least-squares method on F^2_{hkl} in the anisotropic approximation for all non-hydrogen atoms using the SHELXL software [13]. The H(1)–H(4) hydrogen atoms were located objectively from difference Fourier maps and refined in the isotropic approximation. The other hydrogen atoms were placed into geometrically calculated positions and refined in the isotropic approximation using the riding model (U_{iso}(H) = 1.2 U_{equiv}(C)). The main crystallographic characteristics of complex **VIII** are summarized in Table 1.

The full set of X-ray diffraction data for H_2[ZnL(H_2O)]·$2H_2O$ was deposited with the Cambridge Crystallographic Data Centre (CCDC no. 2172274; deposit@ccdc.cam.ac.uk or http://www.ccdc.cam.ac.uk).

RESULTS AND DISCUSSION

Ethylenediaminetetraacetates of divalent metals M[ML]·nH_2O (M = Mn^{2+}, Co^{2+}, Ni^{2+}, Cu^{2+}, Zn^{2+}, Cd^{2+}, Pb^{2+}) are prepared by reactions of suspensions of metal oxides and carbonates with EDTA, or by reactions of water-soluble metal salts with EDTA sodium derivatives [4]. The compounds are poorly soluble in aqueous media. For manganese, the solubility is 0.13 mol/L, while for zinc it is 0.039 mol/L. Zinc derivative **I** reacts with Na_4L to give soluble ethylenediaminetetraacetate zincate **II** [14]:

$$\underset{\textbf{(I)}}{Zn[ZnL]} + Na_4L = \underset{\textbf{(II)}}{2Na_2[ZnL]} \quad (1)$$

Table 1. Crystallographic characteristics and X-ray experiment and structure refinement details for **VIII**

Parameter	Value
Molecular formula	$C_{10}H_{20}N_2O_{11}Zn$
M	409.65
Space group	$C2/c$
a, Å	10.97710(9)
b, Å	9.75975(7)
c, Å	14.56413(13)
β, deg	95.5401(8)
V, Å^3	1553.02(2)
Z	4
ρ(calcd.), g/cm^3	1.752
μ, cm^{-1}	1.644
T, K	298
Crystal size, mm	0.55 × 0.45 × 0.35
F(000)	848
Ranges of h, k, l	$-15 \le h \le 15$, $-13 \le k \le 13$, $-20 \le l \le 20$
$(\sin\theta/\lambda)_{max}$	0.704
Number of reflections: measured/unique	45657/2283
R_{int}	0.0199
Number of parameters	127
S	1.058
R_1/wR_2 (all reflections)	0.0198/0.0572
R_1/wR_2 ($I > 2\sigma(I)$)	0.0204/0.0576
Extinction coefficient	0.0087(5)
$\Delta\rho_{min}/\Delta\rho_{max}$, e/Å^3	0.517/−0.364

The synthesis of compound **I** from zinc oxide and EDTA includes two steps. The first step gives a readily soluble monomeric (or oligomeric) product, which precipitates as large crystals within 10–12 h. Storage of the solution or evaporation of the solution and drying of the residue induce monomer polymerization and afford a poorly soluble compound. Reaction (1) takes place not only for the sodium salt, but also for potassium, ammonium, monoethanolammonium, and hexamethylene-1,6-diammonium salts of EDTA. The derivatives K_2[ZnL] (**III**), $(NH_4)_2$[ZnL] (**IV**), $(H_3NCH_2CH_2OH)_2$[ZnL] (**V**), and $\{H_3N(CH_2)_6NH_3\}$[ZnL] (**VI**) are highly water-soluble.

$$\underset{\textbf{(I)}}{Zn[ZnL]} + \underset{}{(H_3NCH_2CH_2OH)_4\,L} = \underset{\textbf{(V)}}{2(H_3NCH_2CH_2OH)_2[ZnL]} \quad (2)$$

$$\underset{\textbf{(I)}}{Zn[ZnL]} + \underset{}{\{H_3N(CH_2)_6NH_3\}_2L} = \underset{\textbf{(VI)}}{2\{H_3N(CH_2)_6NH_3\}[ZnL]} \quad (3)$$

The tetrakis(triethylammonium) salt of EDTA behaves in a different way. The reaction with Zn[ZnL] does not give the expected bis(triethylammonium) ethylenediaminetetraacetate zincate $\{(C_2H_5)_3NH\}_2$[ZnL], but gives instead mono(triethylammonium) ethylenediaminetetraacetate zincate.

$$Zn[ZnL] + \{(C_2H_5)_3NH\}_4L = 2\{(C_2H_5)_3NH\}H[ZnL] + 2(C_2H_5)_3N. \quad (4)$$

After drying at 110°C, the compound holds one water molecule, being the monohydrate $\{(C_2H_5)_3NH\}H[ZnL]\cdot H_2O$ (**VII**). Its IR spectrum dif-

fers significantly from the spectra of **V** and **VI**, derived from primary amines. Figure 1 shows the IR spectra of **VII** and **VI**. It is known that salts of tertiary amines absorb at 2700–2250 cm^{-1}. In the case of **VII**, this spectral range exhibits a broad intense absorption band. The primary amine salts absorb in even a wider range from 3300 to 2200 cm^{-1}, as can be seen from the spectrum of hexamethylene-1,6-diammonium **VI** derivative. The spectra of these compounds considerably differ in the regions of N–H and O–H stretching (3600–3250 cm^{-1}) and bending (1750–1550 cm^{-1}) modes. A typical feature of the IR spectrum of **VII** is the presence of two strong sharp peaks at 3583 and 3476 cm^{-1}. They cannot be assigned to N–H vibrations. Hence, they are attributable to O–H stretching modes in the coordinatively bound water and free –COO–H group of the acid. The presence of the –COO–H group is confirmed by the band at 1715 cm^{-1} in the O–H bending region. The absorption at 1600 cm^{-1} is due to the C=O stretching modes of the $-COO^-$ carboxylate anion and free COOH group, and N–H bending mode.

An attempt to recrystallize $\{(C_2H_5)_3NH\}H[ZnL]$ from a supersaturated aqueous solution resulted unexpectedly in the synthesis of a new compound: zinc ethylenediaminetetraacetate $H_2[ZnL]\cdot 2H_2O$.

$$\{(C_2H_5)_3NH\}H[ZnL] + 3H_2O = H_2[ZnL(H_2O)]\cdot 2H_2O + (C_2H_5)_3N. \quad (5)$$
(**VIII**)

Zinc complex **VIII** precipitated as large cubic crystals (Fig. 2) containing three bound water molecules. The IR spectrum of **VIII** (Fig. 1) shows a very intense absorption in the region of O–H stretching modes, which corresponds to the three water molecules of crystallization and the –COO–H group. The latter is clearly manifested in the region of O–H bending modes (1712 cm^{-1}).

The formation of crystal structure is a complex process, as follows from SEM data (Fig. 3). The process starts with the appearance of nano- and microcrystals in the solution, which subsequently stick together to form lumps. The crystals that have grown to a large size are imprinted into the lumps (Fig. 3a). It follows from powder X-ray diffraction data that the precipitate almost did not contain an amorphous component (Fig. 4, *3*), which could have acted as a binder for the formation of large agglomerates from small crystals. Apparently, the nanosized structures serve as binders. The isolation of microcrystals from the matrix gives rise to an irregular cellular structure (Fig. 3b) with a cell size of 1.5–2.5 μm. A factor favorable for the success of X-ray experiment is the presence of sufficiently large "free" crystals. At large magnification, it can be seen that they are not monolithic (Fig. 3c). Parallel nanocracks can be detected on their surface.

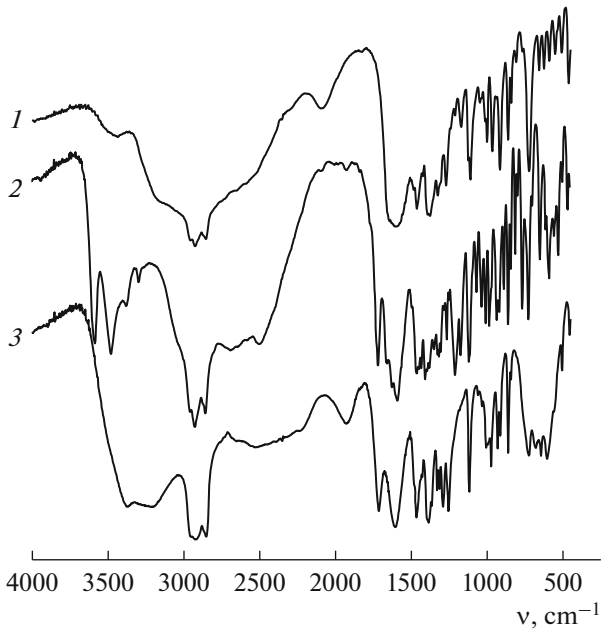

Fig. 1. IR spectra of compounds (*1*) **VI**, (*2*) **VII**, and (*3*) **VIII**.

Compounds **III**–**VIII** were studied by powder X-ray diffraction. 2-Aminoethanol **V** proved to be amorphous, while the other were crystalline. The amorphous nature of **V** was manifested in its behavior. After the synthesis, this was a waxy compound, which puffed up during heating in vacuum. Figure 4 showed the X-ray diffraction patterns of complexes **VI**–**VIII**, from which it follows that they crystallize as different crystallographic types. The amorphous component was virtually absent. Although compound **VI** was highly crystalline, it could not be recrystallized (reprecipitated) from a concentrated aqueous solution by adding dioxane or methanol. Saturation was not attained either. A very high solubility in water was manifested as the formation of a viscous solution converted to a resin. 2-Aminoethanol derivative **V** showed a similar behavior. The solubility of compound **VII** also proved to be very high (10.4 g in 10 mL of H_2O). However, the saturated solution was not stable and induced precipitation of new compound **VIII**.

Aqueous solutions of the zinc complexes were colorless. The UV–Vis spectra of the complexes did not show clear-cut bands in the 250–400 nm range (Fig. 5). Only the solution of compound **VI** was slightly yellowish. The UV–Vis spectrum exhibited an absorption band with a maximum at 280 nm, which

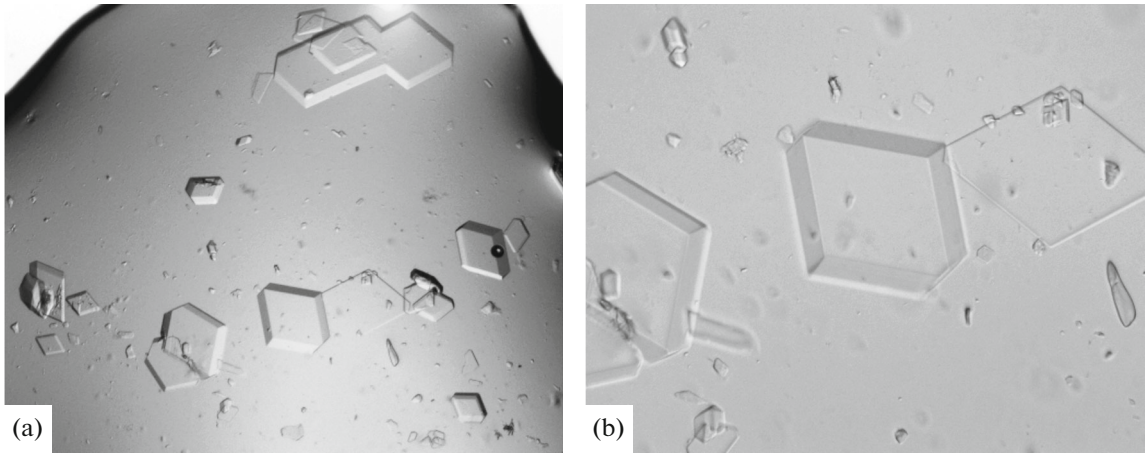

Fig. 2. Optical image of the crystal of **VIII**. Magnification: (a) ×40 and (b) ×100.

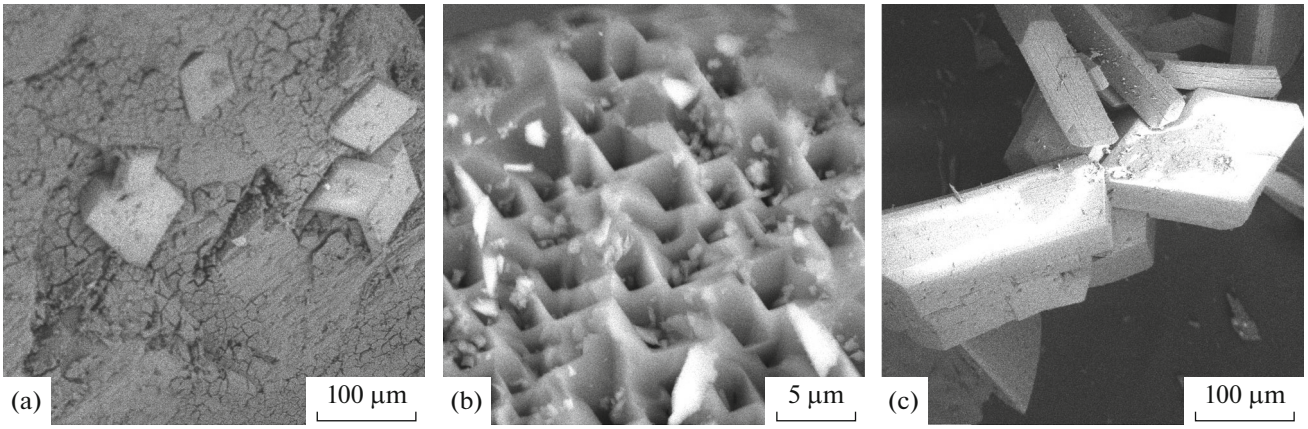

Fig. 3. (a–c) SEM images of the crystals of **VIII**.

extended up to 400 nm with decreasing intensity (Fig. 5, *3*).

As mentioned above, the zinc ion shows no absorption bands in the UV region, since zinc has no characteristic electron transitions in the 3*d*-configuration. The positions of spectral bands of the complexes are determined by the ligand field and depend on the nature of the ligands. In general, the shift tends to be hypsochromic and independent of the nature of the central atom. For this reason, the assignment of the 280 nm band of compound **VI** to the ligand-to-metal transition is unlikely. A possible reason for the appearance of a series of bands in this region is photo- or thermochemical change of the ligand, which may initiate the appearance of impurities during purification of the complex. It is generally known that amines turn yellow under the action of light or heat, since absorption bands appear in the near-UV region. A continuous absorption up to 270 nm is also present (Fig. 5, *2*) for a solution of 2-aminoethanol derivative **V**.

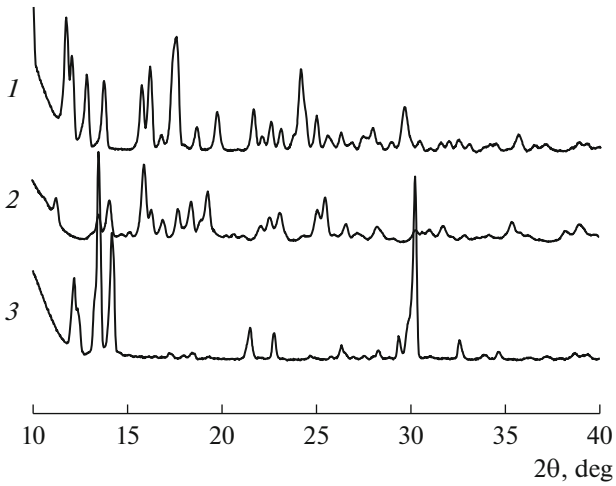

Fig. 4. X-ray diffraction patterns of complexes (*1*) **VI**, (*2*) **VII**, and (*3*) **VIII**.

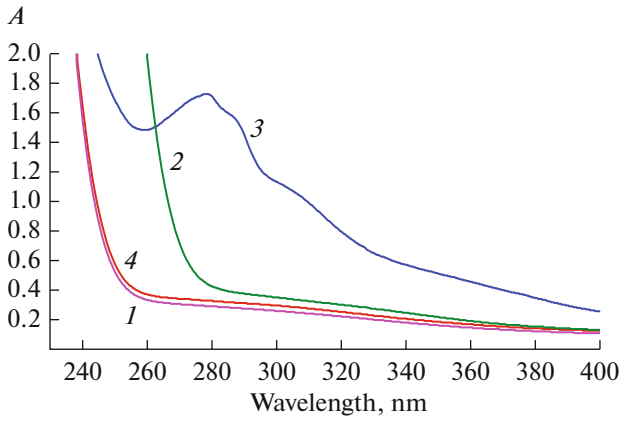

Fig. 5. UV–Vis spectra of zinc complexes with EDTA: (*1*) **IV**, (*2*) **V**, (*3*) **VI**, and (*4*) **VII**, where *c*, mol L^{-1} = 1.2 × 10^{-1}, 4.8 × 10^{-2}, 9.2 × 10^{-2}, and 8.2 × 10^{-2}, respectively.

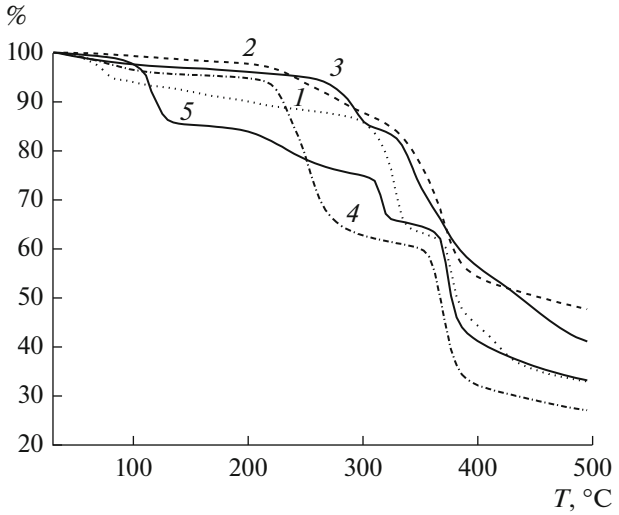

Fig. 6. Thermogravimetric analysis of compounds: (*1*) **IV**, (*2*) **V**, (*3*) **VI**, (*4*) **VII**, and (*5*) **VIII**.

According to thermogravimetric analysis, compounds **IV**–**VI** start to rapidly lose weight only at 290–300°C (Fig. 6). Triethylamine derivative **VII** and the product of its deamination **VIII** are less stable. The weights of the positively charged moiety (NH_4^+, $H_3N^+CH_2CH_2OH$, $H_3N^+(CH_2)_6NH_3^+$, and $(C_2H_5)_3NH^+$) of **IV**, **V**, **VI**, and **VII** are 13, 25, 25, and 25%, respectively (together with H_2O for **IV** and **VII**). This volatile part is completely eliminated by 300, 370, 360, and 260°C. In the low-temperature region (below 150°C), compound **VIII** is least stable. In the 100–140°C range, fast loss of 14% of the weight takes place. In the TGA curve, this step corresponds to the removal of three water molecules. Complex **VII** actively decomposes in two steps, at 220–280 and 350–400°C, to give volatile products. Of all the complexes, it loses the greatest percentage of weight (74%) as a temperature of 500°C has been reached.

The structural relatedness of the series of compounds follows from analysis of their mass spectra. A fairly large number of fragment ions typical of each compound are usually present [3]. There is no full analogy, especially as regards intensities. In this study, we observed a full analogy of the mass spectra for all compounds **I**–**VIII**. This is exemplified in Fig. 7, which shows three mass spectra for markedly chemically different compounds **III**, **V**, and **VIII**. The spectra can fully coincide if, under electron bombardment, the positively charged part of the complex is converted to a neutral molecule (or atom for **I**–**III**) and is not detected. Ionization yielding positively charged groups takes place for the $[ZnL]^{2-}$ core, which is the same for any of the compounds; this results in almost complete coincidence of the spectra. The molecular ion was detected only for complex **VIII**, but its intensity was relatively low. Interestingly, in the case of complex **III**, there was no molecular ion, but the fragment ions $[K_2[ZnL]]^+$ and $[K[ZnL]\cdot H_2O]^+$ were present, although their intensity was also low. For other complexes, no such fragment ions were detected.

Complex **VIII** was isostructural to the previously reported analogue $H_2[FeL(H_2O)]\cdot 2H_2O$ [15]. The independent part of the unit cell contained a half of the molecule of the complex and one solvating water molecule. The ethylenediaminetetraacetate anion was bound to zinc via four oxygen atoms and two nitrogen atoms. In addition, one water molecule was coordinated to the zinc atom (Fig. 8). Thus, the zinc coordination number was seven and the zinc coordination environment was a pentagonal bipyramid. The Zn–O distances to two independent carboxyl groups of the ligand were considerably different (Table 2). The C(1)–O(1) (1.2034(16) Å) and C(3)–O(4) (1.2381(14) Å) distances were markedly shorter than the C(1)–O(2) (1.3045(15) Å) and C(3)–O(3) (1.2728(13) Å) bonds.

Thus, Zn(1)–O(1) (2.4273(12) Å) is a coordination bond, unlike Zn(1)–O(3) (2.0311(8) Å). A similar pattern of bond length distribution in a metal coordination sphere was observed in the related iron complex [15].

In the crystal, the hydrogen atoms of the C(1)O(1)O(2)H(1) carboxyl groups of **VIII** point towards the oxygen atoms of the solvating water molecules. The H(1)...O(6) distance of 1.77(3) Å attests to the presence of a strong intermolecular specific interaction [16]. In turn, water hydrogen atoms are involved in the formation of intermolecular O–H...O interactions with other molecules of the complex (Table 3). The H...O distances vary in the 1.96(2)–2.06(2) Å range; hence, they can also be classified as

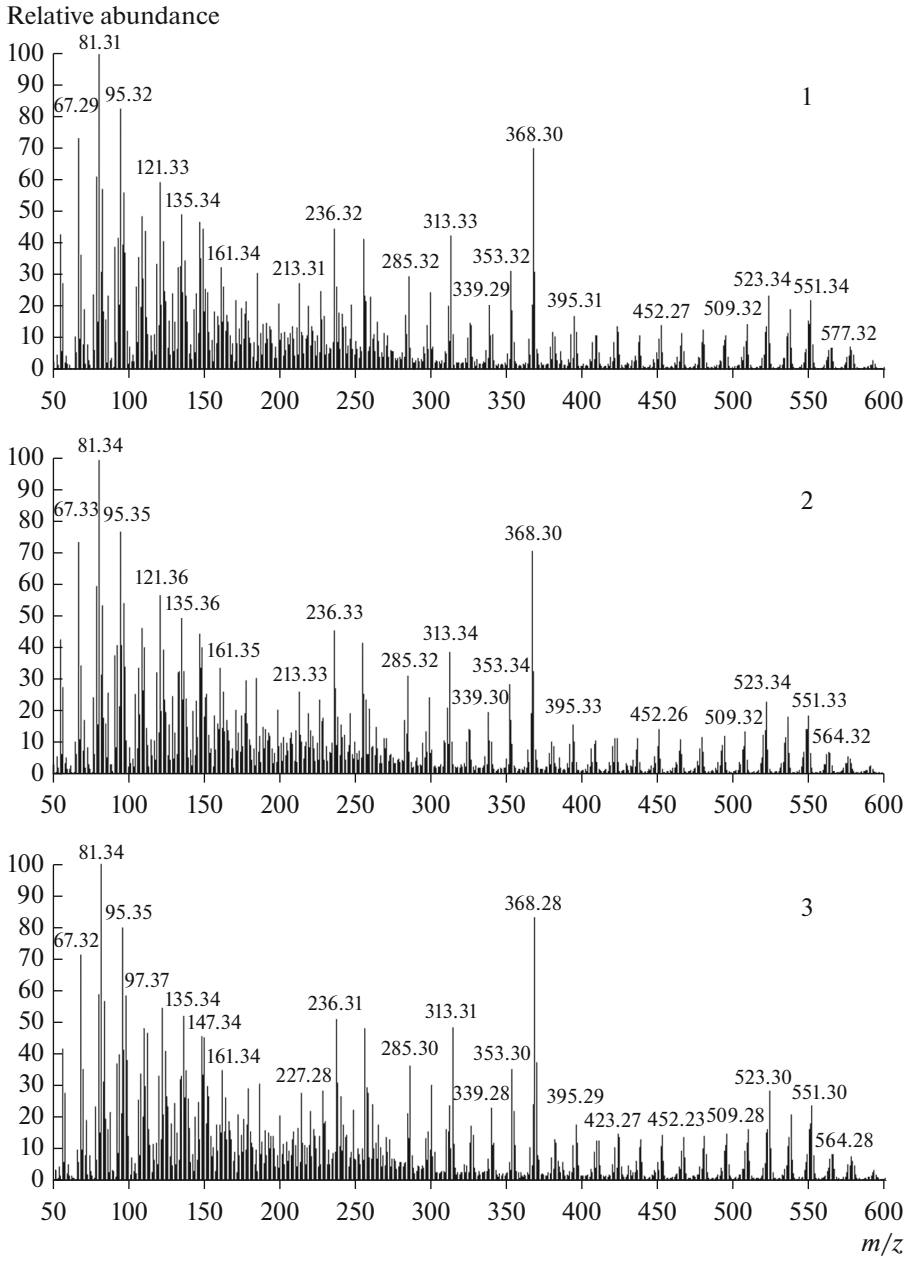

Fig. 7. Mass spectra of (1) $K_2[ZnL]$, (2) $(H_3NCH_2CH_2OH)_2[ZnL]$, (3) $H_2[ZnL(H_2O)]\cdot 2H_2O$.

short contacts [16]. As a result, a 3D network of hydrogen bonds is formed (Fig. 9).

The unusual behavior of **VII** in comparison with derivatives $M_2[ZnL]$ (M = potassium, ammonium, monoethanolammonium, hexamethylene-1,6-diammonium) may be attributable to the presence of free (not anionic) –COOH group in the molecule, resulting in a weakly acidic medium in the solution. In relation to the potassium compound, it was shown that acidification of its aqueous solution did not produce zinc ethylenediaminetetraacetate. Instead, fast precipitation of poorly soluble compound **IX** as finely dispersed particles was observed.

$$\underset{\textbf{(III)}}{K_2[ZnL]} + 0.5H_2SO_4 = \underset{\textbf{(IX)}}{KH[ZnL]} + 0.5K_2SO_4.$$

ACKNOWLEDGMENTS

The study was performed using research equipment of the Center for Collective Use of the Science and Education

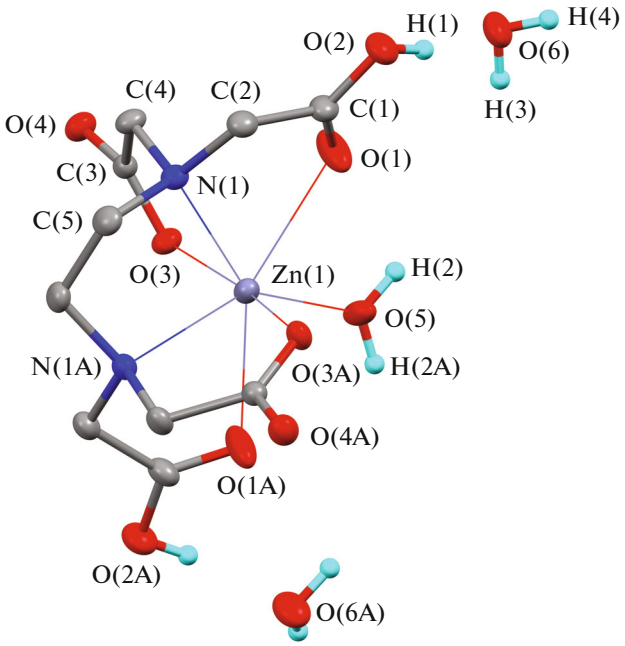

Fig. 8. Molecular structure of complex **VIII**. The thermal ellipsoids are given at 30% probability level. Some hydrogen atoms are omitted for clarity.

Table 2. Selected bond lengths (Å) and bond angles (deg) in complex **VIII**

Bond length, Å	**VIII**	Angle, deg	**VIII**
Zn(1)–O(3)	2.0311(8)	O(3)Zn(1)O(3A)	165.95(5)
Zn(1)–O(5)	2.0376(13)	O(3)Zn(1)O(5)	97.02(2)
Zn(1)–N(1)	2.2715(9)	O(3)Zn(1)N(1)	79.97(3)
Zn(1)–O(1)	2.4273(12)	O(3A)Zn(1)N(1)	89.18(3)
O(1)–C(1)	1.2034(16)	O(5)Zn(1)N(1)	140.38(2)
O(2)–C(1)	1.3045(15)	O(3)Zn(1)N(1A)	89.18(3)
O(3)–C(3)	1.2728(13)	O(3A)Zn(1)N(1A)	79.97(3)
O(4)–C(3)	1.2381(14)	N(1)Zn(1)N(1A)	79.24(5)
N(1)–C(4)	1.4756(14)	O(3)Zn(1)O(1)	89.59(5)
N(1)–C(2)	1.4696(14)	O(3A)Zn(1)O(1)	94.66(5)
N(1)–C(5)	1.4781(15)	O(5)Zn(1)O(1)	72.34(3)
C(1)–C(2)	1.5021(18)	N(1)Zn(1)O(1)	68.16(4)
C(3)–C(4)	1.5251(15)	N(1A)Zn(1)O(1)	147.07(4)
C(5)–C(5A*)	1.519(2)	N(1A)Zn(1)O(1A)	68.16(4)
		O(1)Zn(1)O(1A)	144.69(5)

* Symmetry codes used to generate equivalent atoms in complex **VIII**: (A) $-x + 2, y, -z + 1/2$.

Table 3. Geometric characteristics corresponding to O–H...O contacts in the crystal of **VIII**

D–H...O	Distance, Å			DHO angle, deg
	D–H	H...O	D...O	
O(2)–H(1)...O(6)	0.83(3)	1.77(3)	2.5803(18)	166(3)
O(5)–H(2)...O(4B*)	0.83(2)	1.98(2)	2.7938(12)	169(2)
O(6)–H(3)...O(4B)	0.83(2)	2.06(2)	2.8620(15)	161(2)
O(6)–H(4)...O(3C*)	0.78(2)	1.96(2)	2.7208(13)	167(2)

* Symmetry codes used to generate equivalent atoms in the crystal of **VIII**: (B) $-x + 3/2, y + 1/2, -z + 1/2$; (C) $x, -y + 2, z + 1/2$.

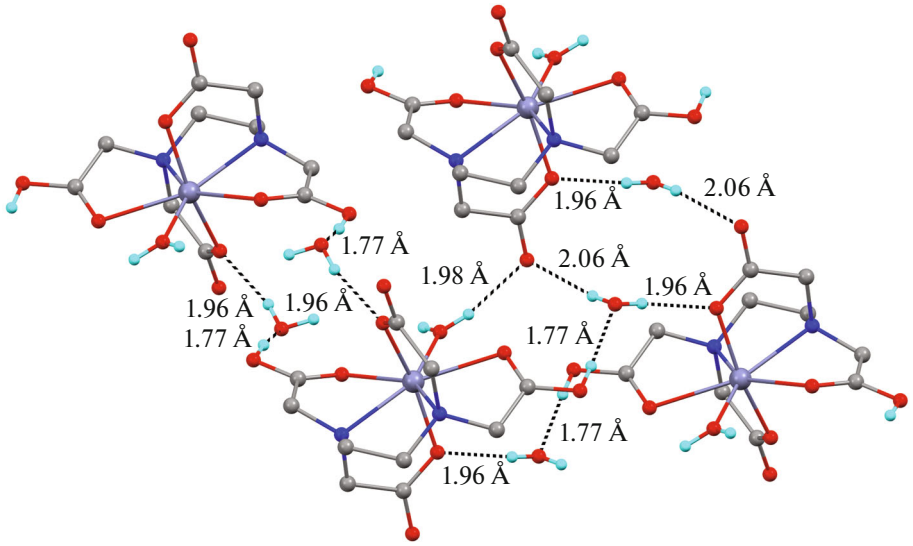

Fig. 9. 3D network of hydrogen bonds in the crystal of **VIII**. Some hydrogen atoms are omitted for clarity.

Center, Physics of Solid-State Nanostructures, at the Lobachevsky State University of Nizhny Novgorod.

FUNDING

The study was performed within the framework of the state assignment (Subject no. 45.4 "Chemistry of Functional Materials," reg. no. 0094-2016-0012) using the equipment of the Center for Collective Use, Analytical Center of the Razuvaev Institute of Organometallic Chemistry, Russian Academy of Sciences, at the Razuvaev Institute of Organometallic Chemistry, Russian Academy of Sciences, and was supported by the grant "Provision of the Development of the Material and Engineering Infrastructure of the Centers for Collective Use of Research Equipment" (unique identifier RF–2296.61321X0017, contract no. 075-15-2021-670). The single crystal X-ray diffraction studies were performed as a part of state assignment (Subject no. 44.2, reg. no. AAAA-A16-116122110053-1). Scanning electron microscopy experiments were performed within the framework of the state assignment of the Institute of Applied Physics, Russian Academy of Sciences, for fundamental research for 2021–2023 in the Subject no. 0030-2021-0025.

CONFLICT OF INTEREST

The authors declare that they have no conflicts of interest.

REFERENCES

1. Dyatlova, N.M., Temkina, V.Ya., and Popov, K.I., *Kompleksony i kompleksonaty metallov* (Chelating Agents and Metal Chelates), Moscow: Khimiya, 1988.
2. Semenov, V.V., Zolotareva, N.V., and Petrov, B.I., RF Patent 2015110362/04, 2017.
3. Semenov, V.V., Zolotareva, N.V., Novikova, O.V., et al., *Russ. Chem. Bull.*, 2022, vol. 71, no. 5, p. 980.
4. Leont'eva, M.V. and Dyatlova, N.M., *Koord. Khim.*, 1990, vol. 16, p. 823.

5. Lakshminarayanan, R., *J. Electrochem. Soc. India*, 1997, vol. 46, p. 45.
6. Borowiec, M., Hoffmann, K., and Hoffmann, J., *Int. J. Environ. Anal. Chem.*, 2009, vol. 89, p. 717. https://doi.org/10.1080/03067310802691672
7. Jervis, R.E. and Krishnan, S.S., *J. Inorg. Nucl. Chem.*, 1967, vol. 29, p. 97. https://doi.org/10.1016/0022-1902(67)80149-0
8. Bampidis, V., Azimonti, G., de Lourdes Bastos, M., et al., *EFSA J.*, 2020, vol. 18, p. e06145. https://doi.org/10.2903/j.efsa.2020.6024
9. Collins, R.N., Merrington, G., McLaughlin, M.J., and Knudsen, C., *Environ. Toxicol. Chem.*, 2002, vol. 21, p. 1940. https://doi.org/10.1002/etc.5620210923
10. Soulages, O.E., Acebal, S.G., Grassi, R.L., and Vuano, B.M., *An. Asoc. Quim. Argent. (1921–2001)*, 1997, vol. 85, p. 261.
11. *Rigaku Oxford Diffraction. CrysAlis Pro Software System. Version 1.171.41.122a*, Wroclaw: Rigaku Corporation, 2021.
12. Sheldrick, G.M., *Acta Crystallogr., Sect. A: Found Adv.*, 2015, vol. 71, p. 3. https://doi.org/10.1107/S2053273314026370
13. Sheldrick, G.M., *Acta Crystallogr., Sect. C: Struct. Chem.*, 2015, vol. 71, p. 3. https://doi.org/10.1107/S2053229614024218
14. Fridman, A.Ya., Leont'eva, M.V., and Dyatlova, N.M., *Koord. Khim.*, 1986, vol. 12, p. 736.
15. Mizuta, T., Wang, J., and Miyoshi, K., *Inorg. Chim. Acta*, 1995, vol. 230, p. 119. https://doi.org/10.1016/0020-1693(94)04311-I
16. Zefirov, Yu.V. and Zorkii, P.M., *Russ. Chem. Rev.*, 1995, vol. 64, p. 415. https://doi.org/10.1070/RC1995v064n05ABEH000157

Translated by Z. Svitanko